

# Water-Soluble Copolymers. 63. Rheological and Photophysical Studies on the Associative Properties of Pyrene-Labeled Poly[acrylamide-co-sodium 11-(acrylamido)undecanoate]

Michael C. Kramer, Cynthia G. Welch, Jamie R. Steger, and Charles L. McCormick\*

Department of Polymer Science, University of Southern Mississippi, Hattiesburg, Mississippi 39406-0076

Received January 17, 1995; Revised Manuscript Received May 4, 1995\*

**ABSTRACT:** The synthesis, rheological, and fluorescence properties of a novel water-soluble polymer based on a micelle-forming monomer are reported. Sodium 11-(acrylamido)undecanoate (SA), a surface-active monomer, copolymerizes readily with acrylamide (AM) to give high molecular weight polymer. Incorporation of the fluorescent monomer [2-(1-pyrenylsulfonamido)ethyl]acrylamide into the monomer feed yields a terpolymer with associative solution properties different from previously synthesized AM/SA copolymers. The fluorescent label acts as a model hydrophobe; changes in associations that elicit a viscosity response in AM/SA copolymers also affect the emission characteristics of the pyrene label. Steady-state fluorescence emission studies reveal significant constriction of the polymer chain as pH decreases or electrolyte concentration increases. As a result, the nature of pyrene-pyrene association can be varied from inter- to intramolecular as electrolyte or acid concentration increases. Fluorescence quenching studies indicate that the salt-induced chain contraction may enhance the organization of mixed polymeric micelles formed by SA and pyrene repeat units. Emission studies of mixed solutions of labeled AM/SA copolymer with surfactants reveal a micellar bridging mechanism. The steady-state emission techniques employed confirm the pronounced pH and salt-responsiveness of AM/SA-based polymers observed in viscosity studies.

## Introduction

Ongoing research in our laboratories involves the synthesis and characterization of water-soluble polymers that exhibit associative behavior in aqueous media. Of particular interest are amphiphilic copolymers containing both hydrophilic and hydrophobic monomers. The pronounced associative thickening behavior observed in these systems arises from interpolymer hydrophobic associations. For example, the viscosity profile of aqueous solutions of copolymers of acrylamide with small levels ( $\leq 1$  mol %) of *n*-alkylacrylamide comonomers possesses an upward curvature at a low critical overlap concentration ( $C^*$ ).<sup>1</sup> This  $C^*$  occurs well below the onset of chain entanglement observed in acrylamide homopolymer. When fluorescent hydrophobes are incorporated into acrylamide polymers, the photophysical response may effectively probe solution behavior on the microscopic level. Copolymers of acrylamide with a pyrene-containing acrylamido monomer exhibit a parallel increase in excited-state dimer (excimer) formation and viscosity.<sup>2,3</sup> Interpolymer hydrophobic associations between pyrene groups that bring about the viscosity response also induce changes in the photophysical behavior.

Ionic group incorporation improves the solubility of these systems, and solution properties can become dependent on pH and/or electrolyte concentration. Terpolymerization of acrylamide, *n*-decylacrylamide ( $C_{10}$ -AM), and a carboxylate or sulfonate acrylamido comonomer affords a copolymer with strong associative properties.<sup>4</sup> The salt- and pH-responsiveness inherent to these systems is a function of ionic group type and placement. Hydrophobic associations in carboxylate-based systems are much stronger than those observed for their respective sulfonate analogs. Also, placement of the ionic group farther from the polymer backbone

appears to affect the nature of the hydrophobic associations.<sup>4</sup>

If a hydrophobic group and a zwitterionic or ionic group are incorporated into the same vinyl monomer unit, water solubility and surface activity can result. Sodium 11-(acrylamido)undecanoate (Figure 1) is one such surface-active amphiphile readily polymerizable by free-radical techniques.<sup>5</sup> Previous studies of SA homopolymer and copolymers with acrylamide (AMSA)<sup>6,7</sup> indicate considerable pH- and salt-responsiveness; pyrene probe studies confirm the formation of micellar microdomains. SA can be described as a "tail-end-attached" monomer.<sup>8,9</sup> The repeat units of the resultant polymer contain a carboxylate group on the end of a pendent hydrophobic group. When this geometry is assumed, the motions of the hydrophobic group are coupled to the polymer backbone, and the pendent polar group may perturb hydrophobic associations in aqueous solution. As a result, polymerized, tail-attached surfactants possess good water solubility and poor micellization.<sup>9</sup> Pyrene probe studies indicate a micellar environment not quite as hydrophobic as that formed by polymerized surfactants containing polar groups closer to the polymer backbone. Similar results are observed for polymerized sodium 11-undecanoate micelles, and restriction of pyrene from efficiently organized polymeric micelles has been postulated.<sup>10-12</sup>

The objective of this study is the elucidation of the associative properties of a terpolymer of acrylamide (AM), sodium 11-(acrylamido)undecanoate (**1**; Figure 1), and the fluorescent label [2-(1-pyrenylsulfonamido)ethyl]acrylamide (**2**; Figure 1). Small incorporations of SA ( $\leq 10$  mol %) and **2** ( $< 1$  mol %) are sufficient to impart unique solution properties. Viscosity studies have shown that domain organization is highly dependent on pH and salt concentration and that SA imparts this responsiveness. Fluorescence emission techniques with an incorporated label allow investigation of the solution properties on the microscopic level. Techniques

\* Abstract published in *Advance ACS Abstracts*, June 15, 1995.

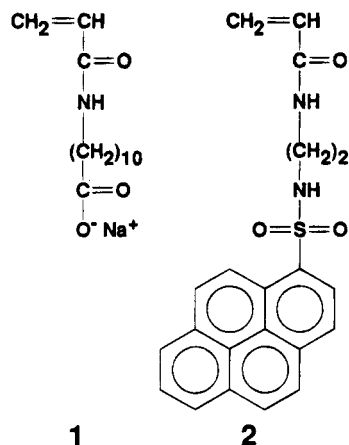


**Figure 1.** Sodium 11-(acrylamido)undecanoate (SA, **1**) and [2-(1-pyrenylsulfonamido)ethyl]acrylamide (APS ("Py"), **2**).

such as these have previously been employed by our research group in studies of naphthalene- and pyrene-labeled water-soluble polymers.<sup>2,3,13-15</sup>

## Experimental Section

**Materials.** All reagents and solvents were purchased from Aldrich Chemical Co. (Milwaukee, WI) unless noted otherwise. Acrylamide was recrystallized twice from acetone. Other materials were used as received. Water for synthesis and solution preparation was deionized and possessed a conductance  $<10^{-7}$  mho/cm.

**Sodium 11-(Acrylamido)undecanoate (SA) (1).** The methods of Gan<sup>5</sup> were employed in the synthesis of SA monomer. Purity was confirmed via NMR and melting point determination.

**[2-(1-Pyrenylsulfonamido)ethyl]acrylamide (2).** The procedure employed by Ezzell and McCormick<sup>2</sup> was followed to give pyrene monomer in good yield and purity according to NMR and HPLC analysis.

**Pyrene-Labeled AM/SA Copolymer (AMSA/Py) (3).** A solution of sodium 11-(acrylamido)undecanoate (1.80 g, 6.5 mmol) and acrylamide (9.00 g, 127 mmol) in 340 mL of H<sub>2</sub>O was added to a reaction flask immersed in a water bath at 50 °C. After finely ground [2-(1-pyrenylsulfonamido)ethyl]acrylamide (0.51 g, 1.3 mmol) was added to the flask, the solution was degassed with nitrogen for 1 h. Sodium dodecyl sulfate (Sigma, 99% pure) (21.7 g, 75.2 mmol) was then added. At this point direct bubbling of nitrogen through the solution was stopped to prevent excessive foaming. The solution was stirred in a nitrogen atmosphere for 3 h; after this time, most, but not all, of the fluorescent comonomer had dissolved into SDS micelles. A degassed solution of potassium persulfate (50 mg, 0.19 mmol) in 5 mL of H<sub>2</sub>O was then injected into the monomer/surfactant solution. After stirring under nitrogen for 3 h, the viscous polymer solution was added to 1400 mL of acetone to yield 7.9 g (70% yield) of a white precipitate. The polymer was washed with refluxing methanol for 16 h in a Soxhlet extractor to remove residual monomer and surfactant.

**Instrumentation.** A Bruker AC-200 NMR spectrometer was used to determine <sup>1</sup>H and <sup>13</sup>C NMR spectra. Molecular weight was obtained with a Chromatix KMX-6 low-angle laser light scattering photometer equipped with a 633-nm HeNe laser. Refractive index increments ( $dn/dc$ ) were measured with a Chromatix KMX-16 laser differential refractometer. UV-vis spectra was recorded with a Hewlett Packard 8452A diode-array spectrophotometer. HPLC was carried out with a Hewlett Packard 1050 Series chromatograph fitted with a photodiode-array UV detector and an Alltech Versapak C<sub>18</sub> reversed-phase column. Steady-state fluorescence spectra were measured with a Spex Fluorolog-2 fluorescence spectrometer equipped with a DM3000F data system. Excitation and emission slit widths of 1 mm, an excitation wavelength of 340 nm, and right angle geometry were employed.

## Results and Discussion

**Polymer Syntheses.** Gan<sup>5</sup> first reported the copolymerization of acrylamide with sodium 11-(acrylamido)undecanoate (SA) at a monomer feed level of  $\geq 30$  mol %. Reactivity ratio studies indicated that SA monomer incorporation was equivalent to the molar ratio of the monomer feed. When a growing radical encounters a micelle containing polymerizable vinyl monomers, the localized monomer concentration and orientation are quite high. Rapid polymerization within the micelle occurs. This is observed as a fast overall polymerization rate yielding high molecular weight polymer. When SA is homopolymerized, high conversion and molecular weight ( $M_w > 10^6$ ) are obtained in a short period of time ( $<1$  h). Even though a low feed level of SA is employed, high conversion within a short period of time is obtained.

Gan reported molecular weights in the  $5 \times 10^5$ – $2 \times 10^6$  range. The molecular weights of AM/SA copolymers are observed to decrease to the lower limit as AM content is increased from 0 to 70 mol %.<sup>6</sup> The AMSA/Py copolymer in our work has a molecular weight of  $1.8 \times 10^6$ . Good monomer, surfactant, and initiator purity may account for the higher molecular weight.

SA incorporation is assumed to equal the monomer feed based on Gan's work and the high conversion obtained. When a copolymer of AM and SA with 90/10 AM/SA (mol/mol) in the monomer feed was characterized by integration of <sup>1</sup>H NMR spectra, a copolymer composition of  $10 \pm 1$  mol % was determined. If stoichiometric SA incorporation is assumed, 0.6 mol % incorporation for AMSA/Py is determined from UV/vis studies ( $\epsilon_{Py} = 24\,100 \text{ M}^{-1} \text{ cm}^{-1}$  at 350 nm). The polymerization utilized 1 mol % fluorescent monomer in the monomer feed, but only 60% of the monomer was incorporated. Ezzell and McCormick<sup>2</sup> also reported low pyrene comonomer content in acrylamide copolymers synthesized both in a homogeneous manner and in the presence of added surfactant. Incomplete pyrene monomer uptake by aqueous SDS micelles may account for this result. After pyrene monomer is added to the aqueous AM/SA/SDS solution, complete dissolution to reattain a clear monomer solution does not occur. Even after several hours of stirring at 50 °C, undissolved fluorescent monomer persists.

The procedure in which an external surfactant is added to copolymerize a hydrophobic monomer with a hydrophilic monomer in aqueous solution is termed "micellar polymerization". This technique can impart unique microstructural characteristics.<sup>16-18</sup> A "blocky" microstructure may result from the inherent heterogeneity of the medium. When such a polymerization is carried out, the propagating radical in aqueous solution adds to the hydrophilic monomers in the aqueous phase. When the macroradical encounters a micelle, polymerization of monomers within the micelle is favored as their residence time in the micelle increases. At high surfactant concentrations, this is a valid assumption, as the polymerization rate ( $k_p$ ) is quite high ( $10^3$ – $10^4 \text{ M}^{-1} \text{ s}^{-1}$ ) for acrylamide and its related monomers.<sup>19</sup> Since virtually all of the hydrophobic monomer, along with a fraction of the acrylamide,<sup>6,20</sup> is partitioned into the micellar interior, a blocky incorporation of hydrophobic monomer is likely. Runs of hydrophobic unit should be separated by long runs of hydrophilic sequences. In aqueous solution, concentration-dependent intra- or intermolecular associations of these hydropho-

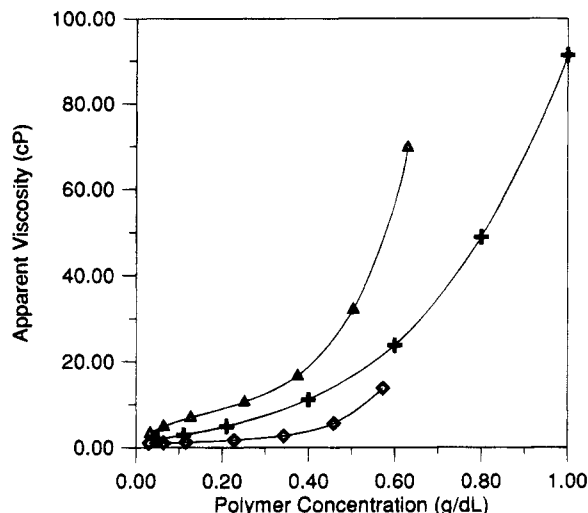


**Figure 2.** Apparent viscosity of poly(acrylamide) ( $(5-6) \times 10^6$ ) as a function of polymer concentration in deionized water (+); apparent viscosity of AMSA/Py ( $1.8 \times 10^6$ ) as a function of polymer concentration in deionized water ( $\Delta$ ) and aqueous 0.3 M NaCl ( $\Diamond$ ). pH 7.

bic segments result in micellelike or associative behavior, respectively.

Recent studies by Zana and Candau<sup>21,22</sup> support the proposed microstructure of these polymers. Surface-active *n*-alkyldimethyl(vinylbenzyl)ammonium chlorides (*n*-alkyl = C<sub>8</sub>, C<sub>12</sub>, and C<sub>16</sub>) were found to polymerize by a nontopological mechanism dependent upon the alkyl chain length. In the case of the C<sub>16</sub> surfactant, radical propagation occurs in nucleated, long-lived micelles that are more stable than unpolymerized micelles. Because the polymerized micelle is more stable than uninitiated micelles, the aggregates grow with the loss of uninitiated aggregates. With surfactants of shorter alkyl chain length, the growing radical does not possess sufficient stability to allow particle growth, and micellar breakdown provides accessibility to the aqueous environment. As the SA concentration in the monomer feed increases, so does the SA micelle concentration; as a result, a higher fraction of SA "blocks" is incorporated into the resultant polymer structure. Because SA is an acrylamido monomer that propagates rapidly, polymerization of most if not all the SA micelle is facile. Chu and Thomas<sup>12</sup> reported the polymerization of sodium 11-undecenoate (SUE) micelles to give oligomers and polymers with molecular weights equivalent to the aggregation number of SUE at a given concentration. The double bond of an acrylamido group would polymerize more rapidly than SUE, and the absence of abstractable hydrogens in the SA monomer structure would eliminate chain transfer as a termination mechanism. Thus, extensive propagation within an SA micelle would effectively compete with micellar breakdown.

**Viscosity and Excimer Emission Studies.** When an AMSA copolymer is labeled with a fluorescent hydrophobe, the apparent viscosity response exhibits a pronounced upward curvature relative to poly(acrylamide) (PAM) of higher molecular weight ( $(5-6) \times 10^6$ ) due to interpolymer hydrophobic association of pyrenyl groups (Figure 2). A low critical overlap concentration ( $C^* \approx 0.35$  g/dL) is observed.  $C^*$  for PAM is 0.6 g/dL. In deionized water above 0.8 g/dL, AMSA/Py solutions possess a gellike, viscoelastic consistency. In 0.3 M sodium chloride, a viscosity reduction indicative of electrolyte-induced coil contraction is observed. Im-

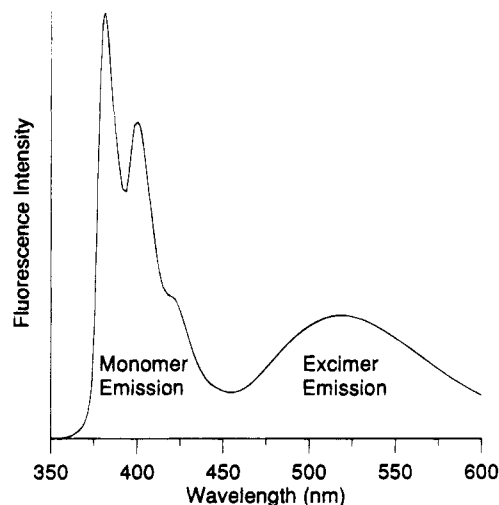


**Figure 3.** Fluorescence emission spectrum of AMSA/Py. Polymer concentration: 0.052 g/dL in deionized water. pH: 7. Pyrene label concentration:  $3.4 \times 10^{-5}$  M. Excitation wavelength: 340 nm.

mediately after addition of sodium chloride to aqueous AMSA/Py solutions, the more highly concentrated ( $>0.2$  g/dL) solutions become gellike with shear-dependent phase behavior; when shaken, the polymer precipitates from solution. Viscosity decreases with time as monomer units reorganize to their most thermodynamically stable conformation.

Viscosity studies provide a reasonable assessment of the bulk, macroscopic solution behavior, but a detailed analysis requires the use of a more sensitive characterization technique. Fluorescence emission studies are inherently sensitive to low chromophore concentrations and angstrom-level motions.

Our research group has investigated pyrene label excimer emission to elucidate solution behavior. As the degree of hydrophobic association increases, interaction between isolated, covalently bound pyrene groups allows the formation of dimeric, sandwichlike conformations that lead to excimer formation. Interpolymer hydrophobic association is observed as an increase in excimer relative to that of "monomer" emission. A typical fluorescence spectrum of AMSA/Py is shown in Figure 3. The peak maxima at 380, 400, and 420 nm arise from the fluorescence emission of isolated pyrenes (monomer emission). The broad, structureless band centered around 520 nm results from emission of excited dimeric pyrene (excimer). The intensity of excimer emission relative to that of the monomer emission ( $I_E/I_M$ ) increases with polymer concentration. This response parallels the macroscopic viscosity behavior.<sup>3,23</sup>  $I_E/I_M$  is plotted as a function of polymer concentration in deionized water in Figure 4.  $I_E$  is taken as the fluorescence intensity at 519 nm and  $I_M$  as the fluorescence intensity at 400 nm.  $I_E/I_M$  steadily increases with polymer concentration. Intermolecular hydrophobic associations between pyrene labels that are responsible for the viscosity profile also increase the population of excited pyrene dimers, and, therefore, there is an increase in  $I_E/I_M$ .  $I_E/I_M$  values for a given polymer concentration are higher in salt. Viscosity studies indicate that the polymer coil shrinks as salt is added. As this occurs, the distance between pyrene groups on the same polymer chain decreases, and excimer formation becomes more favorable. As the polymer concentration increases,  $I_E/I_M$  also increases in 0.3 M NaCl. This seems to indicate that intermolecular aggregation

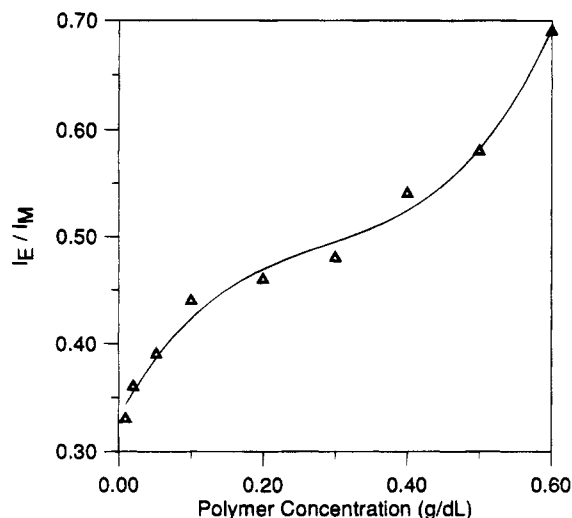


**Figure 4.** Excimer emission/monomer emission ( $I_E/I_M$ ) of AMSA/Py in deionized water. pH: 7.  $I_E$  = fluorescence intensity at 519 nm;  $I_M$  = fluorescence intensity at 400 nm. Excitation wavelength: 340 nm.

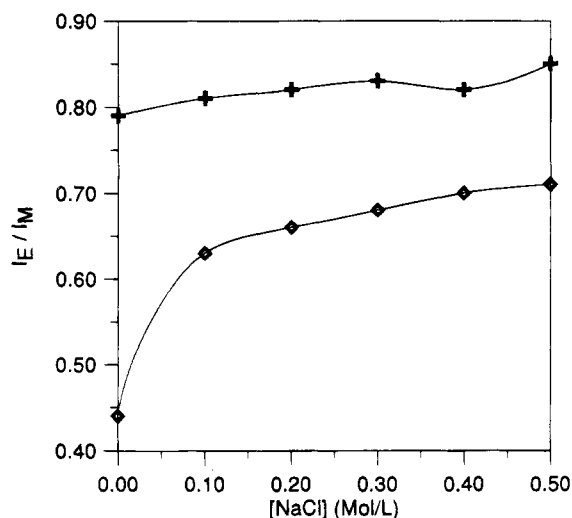


**Figure 5.**  $I_E/I_M$  as a function of aqueous NaCl concentration below ( $\diamond$ , 0.12 g/dL) and above (+, 0.6 g/dL)  $C^*$ . pH: 7.

still occurs although no discernible  $C^*$  in the viscosity response is observed.

Figure 5 illustrates the effects of added electrolyte on the degree of excimer emission below and above the critical overlap concentration ( $C^*$ ). Viscosity studies have shown that a decrease in pH or addition of electrolyte lowers the viscosity of AMSA copolymers. Below  $C^*$ , intrapolymer micellization of SA units is enhanced as charge-charge interactions between pendent carboxylate groups are shielded. Pyrene groups within the polymer coil are closer to one another, and an increase in excimer emission relative to monomer emission is observed. Above  $C^*$ , past the initial onset of polymer-polymer aggregation,  $I_E/I_M$  is independent of ionic strength and polymer concentration. This suggests that pyrene-pyrene aggregation is insensitive to salt above  $C^*$ . This result indicates that interpolymer association occurs primarily via interactions between chromophores.

As can be seen in Figure 6, pH also exerts a considerable effect on polymer dimensions. The viscosity response at pH 4 is considerably less than that at neutral pH for AM/SA copolymer due to protonation of carboxylate groups.<sup>7</sup> At low pH values,  $I_E/I_M$  is quite high, and

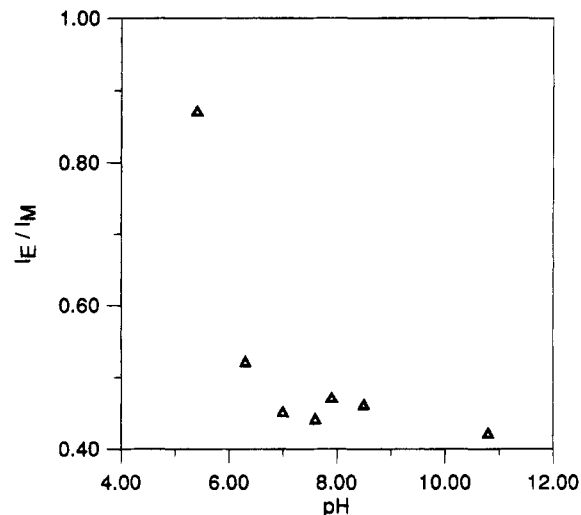


**Figure 6.**  $I_E/I_M$  of AMSA/Py as a function of pH below  $C^*$ . Polymer concentration: 0.12 g/dL.

excimer emission decreases precipitously as the carboxylic acid groups are neutralized. Electrostatic repulsion increases as the degree of ionization along the polymer chain increases. This causes coil expansion and increased separation of pyrenes within individual polymer chains. As pyrene groups become isolated, excimer emission decreases.<sup>23</sup>

**Fluorescence Quenching Studies.** In order to probe ion binding and the accessibility of the pyrenyl-sulfonamido chromophore to the aqueous environment, fluorescence quenching experiments were carried out using the cationic, hydrophilic quencher thallium nitrate ( $TlNO_3$ ) and the amphiphilic quencher nitromethane ( $MeNO_2$ ). First-order quenching constants were calculated using the Stern-Volmer equation.<sup>24</sup> Dynamic, diffusion-controlled quenching can be described as follows:

$$I_0/I = 1 + K_{SV}[Q] \quad (1)$$

$$K_{SV} = k_q\tau_0 \quad (2)$$

where  $I_0$  is the fluorescence intensity of a chromophore in solution in the absence of quencher,  $I$  is the fluorescence intensity at quencher concentration  $[Q]$ ,  $K_{SV}$  is the Stern-Volmer quenching constant ( $M^{-1}$ ),  $k_q$  is the first-order quenching constant ( $M^{-1} s^{-1}$ ), and  $\tau_0$  is the fluorescence lifetime in the absence of quencher. If quenching is dynamic, a plot of  $I_0/I$  vs  $[Q]$  should give a straight line with a slope equal to  $K_{SV}$ .

Stern-Volmer plots for thallium nitrate and nitromethane quenching of 0.12 g/dL of AMSA/Py in deionized water and aqueous sodium chloride solutions are shown in Figures 7 and 8. The linearity of the  $I_0/I$  versus  $[Q]$  plots verifies the dynamic nature of fluorescence quenching. The fluorescence lifetime of the pyrene label was found to be independent of  $[NaCl]$ , so any changes in  $K_{SV}$  would signify changes in quencher-label interactions. From the average (pyrenylsulfonamido)ethyl fluorescence lifetime determined by Ezzell and McCormick<sup>3</sup> ( $\tau_0 \approx 1.3 \times 10^{-8}$  s), quenching rate constants can be calculated. The Stern-Volmer quenching constants and quenching rate constants (Table 1) approximate those of previously reported values.<sup>3,25</sup> The magnitude of the quenching rate constants signifies a dynamic, diffusion-controlled process.

The reduction in the quenching efficiency of  $Tl^+$  with salt addition could arise from enhanced compartment-

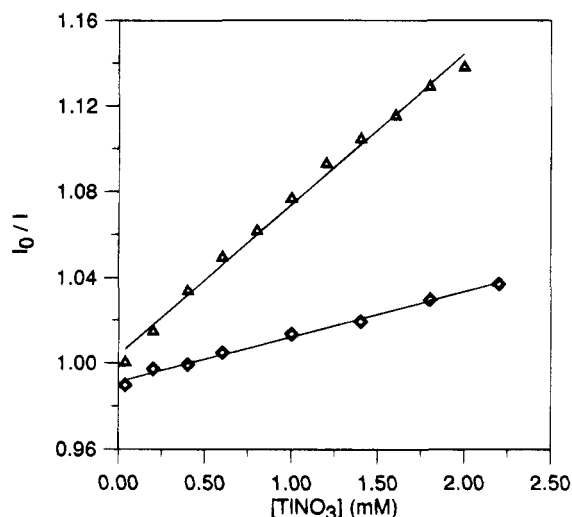


**Figure 7.** Stern–Volmer plot of 0.12 g/dL AMSA/Py quenching by thallium nitrate ( $\text{TlNO}_3$ ) in deionized water ( $\Delta$ ) and in aqueous 0.1 M NaCl ( $\Diamond$ ). pH: 7.  $I$  and  $I_0$  are intensity values at 400 nm.

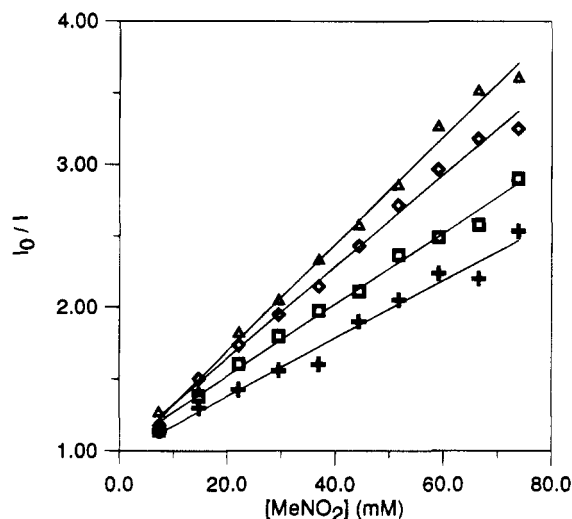


**Figure 8.** Stern–Volmer plot of 0.12 g/dL AMSA/Py quenching by nitromethane ( $\text{MeNO}_2$ ) in deionized water and in  $\text{H}_2\text{O}$  ( $\Delta$ ), 0.1 M NaCl ( $\Diamond$ ), 0.3 M NaCl ( $\square$ ), and 0.5 M NaCl ( $+$ ). pH: 7.  $I$  and  $I_0$  are intensity values at 400 nm.

**Table 1. Fluorescence Quenching of 0.12 g/dL of AMSA/Py in Aqueous Media**

NaCl (M)	$K_{\text{SV}}$ ( $\text{M}^{-1}$ )	$k_q$ ( $\text{M}^{-1} \text{s}^{-1}$ )
Thallium Nitrate		
0	70	$5.4 \times 10^9$
0.1	21	$1.6 \times 10^9$
Nitromethane		
0	35	$2.7 \times 10^9$
0.1	32	$2.5 \times 10^9$
0.3	25	$1.9 \times 10^9$
0.5	20	$1.5 \times 10^9$

talization of pyrene labels as added electrolyte enhances intrapolymer micellization. The reduction is due more likely to dilution of atmospheric  $\text{Tl}^+$  counterions in the presence of added NaCl. At the low molar SA composition in the polymer, the Manning charge density parameter ( $\xi$ ) is less than the critical charge density parameter  $\xi_c$  for univalent counterions ( $\xi_c = 1$ ).<sup>26</sup> If counterions were condensed onto the carboxylate groups, the combination of static quenching by bound  $\text{Tl}^+$  and dynamic quenching by atmospheric  $\text{Tl}^+$  counterions would result in an upward curvature in the Stern–

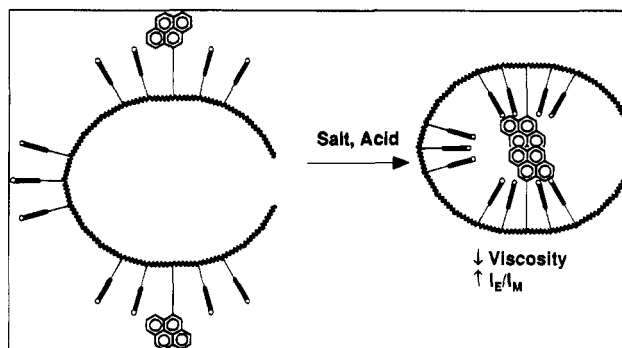


**Figure 9.** Proposed mechanism of salt/pH-triggered collapse of a fluorescently labeled, tail-end-attached polymeric micelle.

Volmer plot. Morishima and Kamachi reported this result for phenanthrene-labeled acrylamide/sodium acrylate terpolymers with varying acrylate anion content.<sup>25</sup> For terpolymer containing 27 mol % sodium acrylate repeat units ( $\xi = 0.67$ ),  $I_0/I$  vs  $[\text{TlNO}_3]$  plots yield a linear response. Higher charge density systems such that  $\xi > 1$  exhibited a nonlinear Stern–Volmer response.

The effect of electrolyte addition on polymer conformation is illustrated by the data obtained from nitromethane quenching studies. Dynamic, diffusion-controlled quenching is indicated by the linear quenching response. As the electrolyte concentration increases,  $K_{\text{SV}}$  decreases. It should be noted that sodium chloride does not quench pyrenylsulfonamide fluorescence. Therefore, it is valid to assume that any change in the nitromethane Stern–Volmer quenching constant with added sodium chloride arises from electrolyte-induced conformational or environmental changes and not from sodium chloride quenching. Ezzell and McCormick<sup>3</sup> determined that pyrene label aggregation had little effect on the quenching constant of nitromethane. For similar concentrations of a random acrylamide/2 copolymer and a similar copolymer with a more blocklike microstructure,  $K_{\text{SV}}$  values did not differ significantly, despite the higher degree of excimer formation observed in the blocky copolymer. In both copolymers,  $K_{\text{SV}}$  values indicated that pyrene labels resided in a rather hydrated environment. If pyrene–pyrene aggregation were the sole association mechanism,  $K_{\text{SV}}$  values would not differ so markedly. Obviously SA micellar structure affects the diffusion of quencher to label. As salt is added,  $K_{\text{SV}}$  decreases. Hydrodynamic diameter also diminishes in this ionic strength regime. The reduction in the probe diffusion rate suggests that the rigidity of SA/Py mixed micelles increases with added salt. This phenomenon is depicted in Figure 9. As acid or electrolyte reduces polymeric micelle dimensions, the shielding (salt) or elimination (acid) of Coulombic interactions between pendent carboxylate groups increases the extent of intramolecular hydrophobic associations.

**Polymer–Surfactant Interactions.** The addition of surfactants to aqueous solutions of amphiphilic polymers can either induce or break up interpolymer aggregation. The nature of the associations is dictated by the surfactant concentration and charge.

Addition of an oppositely charged surfactant such as hexadecyltrimethylammonium chloride (CTAC) to solutions of unlabeled AMSA copolymers results in a dramatic increase in viscosity up to a point where phase separation occurs. When further surfactant is added, AMSA copolymers redissolve, and viscosities decrease. Goddard reported stoichiometric precipitation when

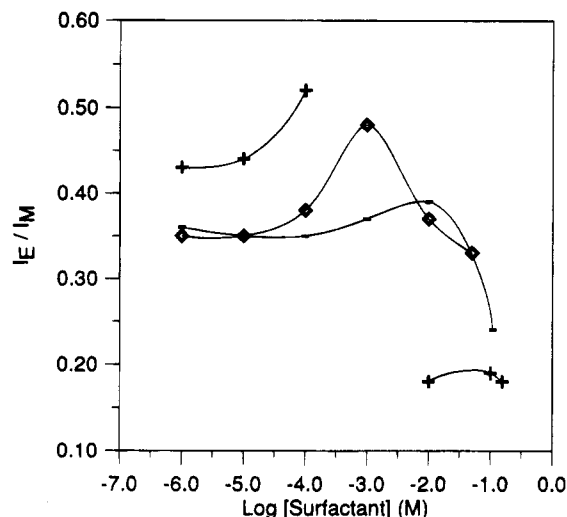


**Figure 10.**  $I_E/I_M$  of 0.12 g/dL AMSA/Py as a function of CTAC (+), SDS (—), and Brij 35 (◇) concentration in deionized water. pH: 7.

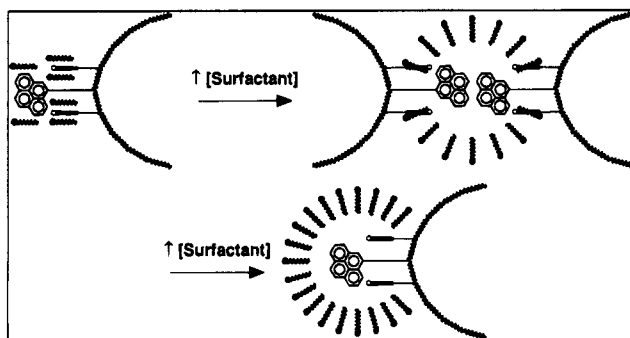


**Figure 11.** Proposed mechanism of polymer-surfactant cross-linking and subsequent aggregate disruption.

anionic surfactant was added to bovine serum albumin on the acidic side of the isoelectric point.<sup>27</sup> Goddard proposed the existence of a second "layer" of bound surfactant ions with the ionic groups pointing outward and the hydrophobic groups associated with the hydrophobic groups of the first layer.<sup>28</sup>

As CTAC concentration is increased in the aqueous solutions of AMSA/Py at neutral pH,  $I_E/I_M$  increases (Figure 10). In the  $10^{-4}$ – $10^{-2}$  M [CTAC] range, the polymer precipitates from solution. The excimer emission enhancement that accompanies increasing viscosity is consistent with an enhancement of interpolymer associations. In a study of the interaction of hydrophobically modified poly(sodium acrylate)s, Iliopoulos reported a viscosity increase and phase separation with increasing dodecyltrimethylammonium chloride (DTAC) concentration.<sup>29</sup> At higher DTAC concentrations, the polymers redissolve. This same trend is observed for AMSA/Py. Iliopoulos proposed a micellar bridging mechanism whereby mixed micelles of surfactant and hydrophobic groups from different polymer chains form transient cross-links. These aggregates are held together by a combination of ionic attractive forces and hydrophobic associations. This mechanism is illustrated in Figure 11. Viscosity then increases as a result of interpolymer aggregation, and phase separation may occur. As further surfactant is added, the hydrophobe/surfactant ratio decreases, and the mixed micelles may contain only a few alkyl side chains due to the disruption of interpolymer cross-links by surfactant (Figure 11). This is reflected in the low  $I_E/I_M$  values exhibited

by AMSA/Py at the high CTAC concentrations where polymer redissolution occurs. Chang and McCormick observed a similar micellar bridging mechanism in solutions of cationic, hydrophobically modified poly(acrylamide)s and the anionic surfactant sodium dodecyl sulfate (SDS).<sup>30</sup>

In mixed solutions of AMSA/Py and an anionic surfactant (SDS) or nonionic surfactant (Brij 35 ( $C_{12}H_{25}-(OCH_2CH_2)_{23}OH$ )),  $I_E/I_M$  displays a maximum (Figure 10). Micellar bridging through hydrophobic associations has been proposed for solutions of hydrophobically modified poly(sodium acrylate)s with nonionic<sup>31</sup> or anionic<sup>32</sup> surfactants. AMSA/Py bridging and aggregate breakup with SDS and Brij 35 would affect the photophysical response. As interpolymer associations are created and then broken up by excess surfactant,  $I_E/I_M$  would increase and then decrease. Similar results have been reported in studies of the interactions of surfactants and phospholipids with pyrene-labeled poly(acrylic acid)s<sup>33</sup> and poly(*N*-isopropylacrylamide)s.<sup>34,35</sup>

## Conclusions

A high molecular weight terpolymer of acrylamide (AM), 5 mol % sodium 11-(acrylamido)undecanoate (SA), and 0.6 mol % [2-(1-pyrenylsulfonamido)ethyl]acrylamide (Py) synthesized by micellar polymerization has been found to exhibit associations dependent upon ionic strength and pH. In deionized water, intermolecular hydrophobic associations through pyrene groups cause a significant viscosity increase. Pyrene-pyrene association is also observed as an enhancement in the degree of excimer emission. The (acrylamido)undecanoate group imparts considerable salt- and pH-responsiveness. As the electrolyte concentration increases or pH decreases, the shielding or elimination of electrostatic repulsions between carboxylate groups shrinks the polymer chain. As the coil dimensions shrink, pyrene groups on the same polymer chain approach one another and excimer emission increases relative to monomer emission. The variability in the photophysical response indicates a salt- or pH-"triggered" mechanism. Interpolymer associations are predominant at low ionic strength and neutral pH. Fluorescence quenching studies reveal that salt-driven coil shrinkage may impart a more restricted, less fluid micellar environment. Maxima in  $I_E/I_M$  values are observed when nonionic or anionic surfactant is added to aqueous AMSA/Py solutions. The addition of cationic surfactant increases  $I_E/I_M$  prior to phase separation. This observation alludes to the presence of a polymer-micelle bridging mechanism proposed by our research group and others.

**Acknowledgment.** Funding from the U.S. Department of Energy, the U.S. Office of Naval Research, and Mobil Oil is gratefully acknowledged.

## References and Notes

- (1) McCormick, C. L.; Nonaka, T.; Johnson, C. B. *Polymer* **1988**, *29*, 731.
- (2) Ezzell, S. A.; McCormick, C. L. *Macromolecules* **1992**, *25*, 1881.
- (3) Ezzell, S. A.; Hoyle, C. E.; Creed, D.; McCormick, C. L. *Macromolecules* **1992**, *25*, 1887.
- (4) McCormick, C. L.; Middleton, J. C.; Cummins, D. F. *Macromolecules* **1992**, *25*, 1201.
- (5) Yeoh, K. W.; Chew, C. H.; Gan, L. M.; Koh, L. L.; Teo, H. H. *J. Macromol. Sci., Chem.* **1989**, *A26*, 663.
- (6) Yeoh, K. W.; Chew, C. H.; Gan, L. M.; Koh, L. L.; Ng, S. C. *J. Macromol. Sci., Chem.* **1990**, *A27*, 711.

- (7) Kramer, M. C.; Welch, C. G.; McCormick, C. L. *Polym. Prepr. (Am. Chem. Soc., Div. Polym. Chem.)* **1993**, *34* (1), 999.
- (8) Laschewsky, A.; Zerbe, I. *Polymer* **1991**, *32*, 2070.
- (9) Laschewsky, A.; Zerbe, I. *Polymer* **1991**, *32*, 2081.
- (10) Sprague, E. D.; Duecker, D. C.; Larrabee, C. E. *J. Am. Chem. Soc.* **1981**, *103*, 6797.
- (11) Paleos, C. M.; Malliaris, A. *J. Macromol. Sci., Rev. Macromol. Chem. Phys.* **1988**, *28*, 403.
- (12) Chu, D. Y.; Thomas, J. K. *Macromolecules* **1991**, *24*, 2212.
- (13) McCormick, C. L.; Chang, Y. *Macromolecules* **1994**, *27*, 2151.
- (14) McCormick, C. L.; Hoyle, C. E.; Clark, M. D. *Macromolecules* **1991**, *24*, 2397.
- (15) McCormick, C. L.; Hoyle, C. E.; Clark, M. D. *Macromolecules* **1990**, *23*, 3124.
- (16) Peer, W. J. *Proc. Am. Chem. Soc. Div. Polym. Mater. Sci. Eng.* **1987**, *57*, 492.
- (17) Turner, S. R.; Siano, D. B.; Bock, J. U.S. Patent 4520182, 1985.
- (18) Branham, K. D.; Davis, D. L.; Middleton, J. C.; McCormick, C. L. *Polymer* **1994**, *35*, 4429.
- (19) *Polymer Handbook*, 2nd ed.; Brandrup, J., Immergut, E. H., Eds.; Wiley: New York, 1975; p II-47.
- (20) Biggs, S.; Hill, A.; Selb, J.; Candau, F. *J. Phys. Chem.* **1992**, *96*, 1505.
- (21) Cochin, D.; Candau, F.; Zana, R. *Macromolecules* **1993**, *26*, 5755.
- (22) Cochin, D.; F.; Zana, R.; Candau, F. *Macromolecules* **1993**, *26*, 5765.
- (23) Kramer, M. C.; Steger, J. R.; McCormick, C. L. *Proc. Am. Chem. Soc. Div. Polym. Mater. Sci. Eng.* **1994**, *71*, 413.
- (24) Lacowicz, J. R. *Principles of Fluorescence Spectroscopy*; Plenum: New York, 1983; Chapter 9.
- (25) Morishima, Y.; Ohgi, H.; Kamachi, M. *Macromolecules* **1993**, *26*, 4293.
- (26) Manning, G. S. *Acc. Chem. Res.* **1979**, *12*, 443.
- (27) Goddard, E. D. *Colloid Surf.* **1986**, *14*, 301.
- (28) Goddard, E. D.; Pethica, B. A. *J. Chem. Soc.* **1951**, 2659.
- (29) Magny, B.; Iliopoulos, I.; Zana, R.; Audebert, R. *Langmuir* **1994**, *10*, 3180.
- (30) Chang, Y.; Lochead, R. Y.; McCormick, C. L. *Macromolecules* **1994**, *27*, 2145.
- (31) Iliopoulos, I.; Olsson, U. *J. Phys. Chem.* **1994**, *98*, 1500.
- (32) Iliopoulos, I.; Wang, T. K.; Audebert, R. *Langmuir* **1991**, *7*, 617.
- (33) Arora, K. S.; Hwang, K.-C.; Turro, N. J. *Macromolecules* **1986**, *19*, 2806.
- (34) Winnik, F. M.; Ringsdorf, H.; Venzmer, J. *Langmuir* **1991**, *7*, 912.
- (35) Ringsdorf, H.; Venzmer, J.; Winnik, F. M. *Angew. Chem., Int. Ed. Engl.* **1991**, *30*, 315.

MA9500502